JOURNAL OF GEOPHYSICAL RESEARCH, VOL. 102, NO. D25, PAGES 29,779–29,788, DECEMBER 27, 1997

Toward monitoring the tropospheric temperature by means of a general circulation model

Martin Stendel and Lennart Bengtsson
Max-Planck-Institut für Meteorologie, Hamburg, Germany

Abstract. The recent global tropospheric temperature trend can be reproduced by climate models that are forced only by observed sea surface temperature (SST) anomalies. In this study, simulations with the Hamburg climate model (ECHAM) are compared to temperatures from microwave sounding units (MSU) and to reanalyses from the European Centre for Medium-Range Weather Forecasts. There is overall agreement of observed and simulated tropospheric temperature anomalies in many regions, in particular in the tropics and over the oceans, which lack conventional observing systems. This provides the opportunity to link physically different quantities, such as surface observations or analyses (SST) and satellite soundings (MSU) by means of a general circulation model. The proposed method can indicate inconsistencies between MSU temperatures and SSTs and has apparently done so. Differences between observed and simulated tropospheric temperature anomalies can partly be attributed to stratospheric aerosol variations due to major volcanic eruptions.

1. Introduction

Human activities are changing the composition of the atmosphere. The concentration of CO_2 has increased 28% (with a current annual trend of +0.5%) from the preindustrial level. Together with the other absorbing gases: methane, nitrous oxide, chlorofluorocarbons (CFCs), etc., the total greenhouse effect can be expressed as an increase in the longwave forcing by ~2.7 W m^{-2} from the beginning of industrialization to the present [*Intergovernmental Panel on Climate Change (IPCC)*, 1996].

Temperature above the surface layer is particularly important in the current global change discussion, since from the Clausius-Clapeyron equation it follows that in a warm atmosphere a moist adiabate will slope less with height than in a cold one, leading, with enhanced greenhouse effect, to a greater temperature rise in the middle troposphere than at the surface [*Manabe et al.*, 1991; *Boer et al.*, 1992]. This is known as the lapse-rate feedback. A large part of the uncertainty related to the detection of the anthropogenic climate signal arises from the fact that longer-term climate records are generally confined to the land surfaces of the extratropics, mostly in the northern hemisphere. Observational data for the troposphere and stratosphere are particularly problematic, with reliable global records only since 1979, though radiosonde measurements at various sites go back to the 1940s.

A comprehensive set of global temperatures comes from polar-orbiting satellites, having the advantage of global data coverage, and giving an estimate, in integral form, of the temperature of the whole troposphere and the lower stratosphere. *Spencer and Christy* [1992a, b] have introduced a method to monitor the temperature of the atmosphere in which the intensity of upwelling microwave radiation as measured by the National Oceanic and Atmospheric Administration (NOAA) polar-orbiting satellites is converted into temperature. Oxygen molecules act as blackbody radiators near the 60-GHz frequency, and their emissions are recorded by the microwave sounding units (MSUs) on board the satellites. *Christy* [1995] has undertaken a comprehensive validation of comparing them with two sets of radiosonde observations for deep layers compiled by *Angell* [1988] and *Oort and Liu* [1993] He showed that the MSU data, when averaged in space and time, are comparable in accuracy to radiosonde observations (see Table 1).

In order to predict climate system changes, general circulation models (GCMs) have been employed. However, the various parts of the climatic system have vastly different equilibrium times, ranging from hours to millennia, and are coupled by numerous nonlinear feedback mechanisms. Nevertheless, GCMs, when forced only with observed sea surface temperature (SST), are able to reproduce the global temperature record [*Graham*, 1995], and they can render the observed large-scale response patterns due to El Niño and La Niña realistically [e.g., *Lau*, 1985; *Hoerling et al.*, 1992], since the tropical circulation is strongly determined by the equatorial Pacific SST anomaly pattern and the interactions with the atmosphere are essentially linear.

In the extratropics the atmospheric circulation is modulated more weakly by both tropical and midlatitude SST anomalies, owing to the nonlinear character of the interactions. On the basis of the work by *Bjerknes* [1964], who showed that interannual SST variability in the North Atlantic is connected to the response of the ocean mixed layer to local ocean-atmosphere heat exchange, several studies point out that interannual SST fluctuations are forced by changing wintertime atmospheric circulation patterns [e.g., *Wallace et al.*, 1990; *Cayan*, 1992a, b]. There is empirical evidence [*Kushnir*, 1994] that atmospheric anomalies in the North Atlantic region precede ocean anomalies on an interannual timescale [see also *Pedersen et al.*, 1990].

Owing to the nonlinearity of the circulation in the extratropics, ensemble experiments that differ only in their initial conditions provide not only some insight into the governing physical processes, but also can show limits for potential predictability. Recently, *Bengtsson et al.* [1996] made such an investigation for basic meteorological quantities in various regions of the Earth. In

Paper number 97JD01668.
0148-0227/97/97JD-01668$09.00

Table 1. Correlations Between Global Anomalies of Tropospheric and Stratospheric Temperatures

	Annual Average	Seasonal Average
	Oort and Liu [1993]	
Troposphere (T_{2R})	0.95	0.91
Stratosphere (T_4)	0.97	0.93
	Angell [1988]	
Troposphere (T_{2R})	0.94	0.80
Stratosphere (T_4)	0.90	0.88

T_{2R} and T_4 refer to microwave sounding unit (MSU) brightness temperatures, and *Oort and Liu* [1993] and *Angell* [1988] to two sets of radiosonde observations. Periods of comparison are MSU / *Oort and Liu*: 1979-1989, and MSU / *Angell*: 1979-1994. From *Christy* [1995].

this study, however, comparisons are not conducted on distinct levels (as in the work of *Bengtsson et al.*, [1996]), but rather, the average temperature of the whole troposphere will be investigated. An ensemble of five forecasts with identical SST as lower boundary forcing, but different atmospheric initial conditions, will be investigated. An attempt is made to combine information from both the MSU temperatures and the SST distribution to study the climate variations of the past 2 decades. Although these are different physical quantities, it is possible to compare them via the model, as will be shown. The results are verified against European Centre for Medium-Range Weather Forecasts (ECMWF) reanalyses for the period 1979 to 1993.

El Niño-Southern Oscillation (ENSO) events are not the only phenomenon that modulate atmospheric temperatures on an interannual scale. Part of the observed temperature changes may also be due to aerosols from large volcanic events that reduce solar heating of the Earth's surface by reflecting sunlight into space, as was recognized more than 200 years ago [*Franklin*, 1784]. Major volcanic eruptions inject large amounts of particles including sulfate aerosol into the stratosphere. Owing to trapping of the outgoing thermal radiation from the Earth's surface and increased shortwave absorption, the stratosphere warms. Two volcanic events occurred since 1979 that have had global impact, the eruption of the Mexican volcano El Chichón (17°N, 93°W) in April 1982 and the eruption of Mount Pinatubo on the Philippine Islands (15°N, 120°E) in June 1991, the latter being the largest such event in this century, as judged from both the amount of ejecta and the plume height [e.g., *Labitzke and McCormick*, 1992]. Accordingly, the lower stratospheric brightness temperature is dominated by marked warmings due to the eruptions of these volcanoes [see *Christy*, 1995]. Since there is no stratospheric aerosol in the model version used here, the model stratospheric temperature is unable to reproduce this curve, and thus will not be discussed further. In addition to ENSO and volcanoes, there may be other factors contributing to interannual temperature variations, both internal (due to complex interactions between the climate system's components) and external, such as by solar variability changes.

The structure of this paper is as follows. In section 2 the characteristics of temperature retrieval by means of the MSU are summarized. Section 3 describes the design of the experiment. An investigation of the model response to forcing by SST anomalies follows in section 4. The potential of regional predictability is addressed in section 5, and a discussion of the results follows in section 6. Finally, some conclusions are drawn.

2. Retrieving Tropospheric Temperatures With Microwave Sounding Units

In the past, monitoring the Earth's temperature was almost exclusively restricted to the surface and to the extratropical land masses of the northern hemisphere. Radiosondes and pilot balloons have been available since the 1940s. However, it was not until 1979 that reliable quantitative satellite observations of temperature covering the whole globe became available.

Satellite upper air temperature is retrieved operationally by NOAA polar-orbiting satellites carrying microwave sounding units that measure the intensity of the upwelling microwave radiation. There are four channels in the MSU, centered near 60 GHz (about 5 mm wavelength), recording the emission of molecular oxygen from deep vertical layers. Since oxygen is an abundant, uniformly mixed gas whose concentration is constant in time, it serves as a good temperature tracer for climate purposes. Emissions from the whole depth of the atmosphere reach the MSU, but by selecting the spectral intervals near 60 GHz, the level of maximum emission can be chosen. Lower stratospheric temperatures can be obtained by MSU channel 4 (57.95 GHz), whose weighting function peaks at 70 hPa, and tropospheric temperatures by channel 2 (53.74 GHz). Since part of the radiation in channel 2 also emanates from the lower stratosphere, a synthetic channel 2R temperature, T_{2R}, composed of eight view angles of channel 2, is used instead [*Spencer and Christy*, 1992b]. With a maximum weighting function near 700 hPa, MSU 2R generally represents the temperature of the lower troposphere.

Since 1979, approximately 24000 observations per day have been available, usually from two satellites in operation at the same time [*Christy et al.*, 1995]. The diurnal cycle is removed by constructing anomalies from an annual cycle, taking into account the equator-crossing time of the satellite [*Spencer and Christy*, 1992a, b, 1993]. A detailed description of how the final time series is obtained from the satellites in use since 1979 is given by *Christy et al.* [1995]. For the derivations of temperature trends the intersatellite stability of the MSU data plays a key role. Global monthly mean temperatures are reproducible within 0.02 K in the stratosphere [*Spencer and Christy*, 1993; *Christy and Drouilhet*, 1994] and 0.04 K in the lower troposphere [*Christy et al.*, 1995]. However, problems occurred due to sensor drift of the sounders on board NOAA 11 and NOAA 12. The correction is discussed in detail by *Christy* [1995].

A potential problem is the part of the signal that is due to non-oxygen emission. Possible sources of contamination of the signal include the following. (1) The influence of precipitation-size ice particles in deep convection (above 400 hPa) can yield cold biases of several degrees, but they play only a minor role for channel 2 [*Prabhakara et al.*, 1996b] and can be screened out due to their isolated nature [*Spencer et al.*, 1990]. (2) The effect of surface emissions can have noticeably large values in mountainous regions but can be eliminated if this effect is systematic [*Spencer and Christy*, 1992a]. This might be not the case in some regions, and such signals will contaminate the MSU record, especially over land. Owing to the method by which the MSU T_{2R} data are obtained, they are noisier than the raw MSU T_2 record. Modifications in surface emissivity due to local changes in vegetation, soil moisture, wind speed, etc., will therefore be reflected more in the T_{2R} than in the T_2 record and make the MSU 2R less reproducible between different satellites [*Spencer and Christy*, 1992b]. In particular, horizontal gradients are weakened by the computation procedure. (3) Cloud water and water vapor may have an effect in tropical regions [*Prabhakara et al.*, 1995, 1996a, b], but they are

estimated to be generally small [*Christy*, 1995; *Spencer et al.*, 1996]. (4) Oceanic surface wind variations are another possible source.

The problem of missing MSU data is mainly confined to the period prior to September 1981. Brightness temperatures for a specific location are generally obtained twice daily, but there are missing MSU observations in November 1979 and April and August 1981. Since there are 15 consecutive days missing in March and April 1981, this may lead to some aliasing of the annual cycle in the extratropics. With the exception of the periods February 1980 to January 1981 (NOAA 6), April 1983 to December 1984 (NOAA 7), and April 1987 to September 1988 (NOAA 10), there were two satellites available to construct the brightness temperatures. However, a global data coverage is granted even with only one satellite.

The MSU data sets have been extensively compared to conventional observations. In the troposphere there is a high correlation between MSU brightness temperatures and vertically weighted radiosonde temperature profiles for both seasonal and annual averages (see Table 1). The correlation coefficient of the MSU data for the data set compiled by *Oort and Liu* [1993] is slightly larger (0.91 on a seasonal basis, 0.95 for annual means) than that from *Angell*'s [1988] investigation (0.80 and 0.94, respectively). This is probably due to the fact that there is insufficient regional coverage in the latter data set [*Christy*, 1995]. The rms differences of monthly MSU anomalies and individual vertically weighted radiosonde temperature profiles range from 0.1 K in the tropics to 0.2 K at high latitudes [*Hurrell and Trenberth*, 1992]. It must, however, be kept in mind that radiosonde observations and MSU data cannot be strictly compared for large area averages, owing to the small number of upper air observations over large parts of the tropics and the southern hemisphere.

Trenberth et al. [1992] compare tropospheric MSU T_2 temperatures with a near-global monthly mean surface temperature data set used by the *IPCC* [1992, 1996]. Although the microwave sounders measure a different physical quantity than observed at the surface and changes in data coverage contribute to noise in the surface data set, the correlation between both is in excess of 0.8 over large parts of the Earth for monthly means. Moderate correlations (~0.5) are found over the tropical and subtropical land areas, while there is only poor correlation over parts of the southern oceans and the tropical western Pacific. The low correlations can be attributed to the vertical structure of temperature anomalies, since pervasive inversions like the tropical trade wind inversion effectively decouple the boundary layer from the free atmosphere. On the other hand, circulation anomalies in high- and middle-latitude land areas are found to have a quasi-barotropic vertical structure in the monthly averaged atmosphere, so that anomalies are highly coherent, despite the shallow inversions that are often found in winter.

One way to overcome the difficulties that arise from different data coverage and from physical differences between surface temperatures and upper air temperatures is to compare the MSU brightness temperatures to meteorological analyses. However, operational analyses are not well suited for this purpose, since they have been more or less by-products of the operational weather forecasts and suffer from the running improvements in model representation, analysis scheme, and variability in data sources that result in inconsistencies. It has therefore been suggested that global atmospheric data should be analyzed with a frozen data assimilation scheme [*Bengtsson and Shukla*, 1988], and several weather services have recently carried out such reanalyses. Data from the ECMWF reanalysis for the period 1979 to 1993 are included in this investigation. The ECMWF reanalyses are not independent of the MSU brightness temperatures. Raw radiances are not directly incorporated into the analysis system, but MSU data are included in clear and partly cloudy retrievals, while in cloudy regions the retrievals depend entirely on MSU data [*Hurrell and Trenberth*, 1992] for regions lacking radiosonde measurements. The MSU and reanalysis are, in fact, most independent over well-observed continental areas, where the radiosonde data supply the upper atmospheric information for the reanalyses. Operational "satellite data" utilized over the oceans in the reanalysis are a combination of many infrared and MSU channels and do not follow the strict intercalibration procedure of the *Spencer, Christy* [1992a, b; 1993] MSU data. Therefore it is entirely possible to find greater differences between the MSU data and reanalysis data over the oceans, where satellite data are employed, than over other regions, where only radiosonde data are utilized.

In summary, MSU brightness temperatures appear to be a suitable tool for monitoring temperature variations on a global basis. With the exception of some missing periods in the first years they are available for the period from 1979 until the present.

3. Experimental Setup

This study has been conducted with ECHAM3, the third-generation atmospheric GCM at the Max Planck Institute for Meteorology [*Roeckner et al.*, 1992], which is based on the ECMWF numerical prediction model. The dynamic fields are represented in terms of spherical harmonics with triangular truncation at a specified wavenumber. For the purpose of this study a truncation of T42 with 19 vertical hybrid levels was chosen, making the spatial scale comparable to that of the MSU data (2.5° x 2.5°). The time step is 24 min.

The atmospheric response to the evolution of SST from 1979 to 1993 is studied. This period is a suitable test period, since there were three fully developed warm events (El Niño) in 1982 / 83, 1986 / 87 and in 1991 / 92 and two cold events (La Niña) in 1985 and 1989. For the period 1979 to 1988, the Atmospheric Model Intercomparison Project (AMIP) data set [*Gates*, 1992] was used, which was created for the intercomparison of atmospheric models

Table 2. Normalized MSU T_{2R} Weighting Coefficients for ECHAM With a Surface Pressure of 1000 hPa

Pressure Level, hPa	Weighting Coefficient
10	0.000
30	0 000
50	0.000
70	-0.002
100	-0.003
150	0.000
200	0.008
250	0.021
300	0.040
400	0.080
500	0.127
700	0.159
850	0.151
900	0.147
950	0.140
Surface	0.132

ECHAM is the Hamburg general circulation model, which is based on the numerical prediction model of the European Centre for Medium-Range Weather Forecasts (ECMWF).

under reproducible conditions. From 1989 to 1993, the SST was obtained from the National Meteorological Center / Climate Analysis Center (NMC / CAC) [*Reynolds*, 1988]. An ensemble of five different integrations with ECHAM3 was performed that are forced with identical monthly means of SST from these data sets, but with slightly different initial atmospheric conditions that were obtained from the control run of the model, which was forced by a climatological mean SST. Results are shown for the individual realizations as well as for the ensemble-averaged response. This allows for an assessment of the internal variability of the model. The results are compared to both the independently obtained MSU brightness temperatures and ECMWF reanalyses for the period 1979 to 1993.

4. The Model Response to SST Anomalies

In order to be comparable to the MSU measurements, the model temperatures are subject to the inversion of the appropriate MSU channel-weighting functions. However, *Spencer and Christy* [1992a] pointed out that because the temperature dependence of variations in both oxygen and water vapor absorption is small, a static weighting function for the U.S. Standard Atmosphere can be applied to obtain a vertically weighted brightness temperature estimate instead of solving the full radiative transfer equation. The temperature anomalies obtained this way differ by less than 0.02 K from the exact values. (Calculation of the absolute brightness temperatures requires the full radiation model, as substantial biases can be created from the neglect of surface emissions in the simple weighting function profile, as pointed out by *Shah and Rind* [1995].) The authors therefore recommend this simple method for quantitative comparisons to multiple-layer data sets, such as the model output. Upwelling radiation from the ground accounts for part of the radiation received in T_{2R} (less than 10% over ocean, up to 20% over land), so that 80% to 90% of the T_{2R} signal stems from the troposphere (see Table 2).

Table 3 shows a regional statistical analysis between MSU T_{2R} and the average of the five ECHAM simulations. The areas were chosen according to *Christy* [1995]. The correlation for annual means is near or above 0.8 for large parts of the globe, with largest values in the tropical east Pacific. For periods undisturbed by volcanic aerosol (see discussion below), the correlations are near 90% throughout the tropics, and high values are also found over the extratropical ocean basins. Owing to the larger variability, correlations based on monthly means are smaller in the extratropics, especially over the Eurasian and North American land masses. This means that for large parts of the globe, correlations are comparable in magnitude to those from other measuring systems (as discussed above: see Table 1).

The correlation of MSU temperatures and ECHAM simulations from the control run, using climatological SST, is practically zero in the tropics (not shown), indicating the importance of the SST anomaly patterns for the state of the atmosphere in this region. SST anomalies play a less important role in the European-Atlantic sector, as shown by *Bengtsson et al.* [1996].

These findings suggest that the main signal for global temperature anomalies comes from the tropical Pacific SST. While this is well known for observations [e.g., *Newell and Weare*, 1976a, b; *Pan and Oort*, 1983; *Angell*, 1990], the ability of ECHAM to reproduce this pattern is investigated in detail by a simulation that uses observed SST anomalies in the tropical Pacific only and climatological SST elsewhere. The results are displayed in the last four columns of Table 3. We find that the model temperature distribution in the tropics is, to a large extent, dominated by tropical Pacific SST anomaly forcing, but there are also extratropical regions, in particular North America, where a relatively large part of the temperature variance can be explained by SST anomalies in the tropical Pacific. *Bengtsson et al.* [1996] give a possible explanation for the mechanism.

The stratospheric temperature record (not shown) is dominated by marked warmings after the eruptions of El Chichón and Mount Pinatubo. Aerosol particles, e.g., from volcanic origin, not only warm the stratosphere, but also scatter sunlight, so that less solar radiation reaches the troposphere. The global tropospheric temperature anomaly pattern (T_{2R}, Figure 1) is influenced by both the ENSO and volcanic signal. In times of undisturbed atmospheric conditions (i.e., in the absence of volcanic aerosol) the temperature difference between the model (forced with observed SSTs) and satellite data does not exceed 0.1 K. However, ECHAM tem-

Table 3. Statistical Regional Comparisons of Temperature Anomalies Between MSU T_{2R} and ECHAM3 model simulations.

Area	Boundaries φ S	φ N	λ W	λ E	Correlation ECHAM3 / MSU_{2R} Annual Average 1979-1993	Annual Average 1983-1991	Monthly Average 1979-1993	Monthly Average 1983-1991	rms, K Annual Average	rms, K Monthly Average	Explained Variance, % Annual Average 1979-1993	Annual Average 1983-1991	Monthly Average 1979-1993	Monthly Average 1983-1991
Globe					0.77	0.98	0.61	0.77	0.08	0.14	50	65	26	34
Land	-90	90	-180	180	0.51	0.87	0.30	0.48	0.15	0.27	18	20	7	7
Ocean					0.78	0.95	0.61	0.76	0.08	0.14	66	83	43	52
Northern Hemisphere	0	90	-180	180	0.80	0.94	0.55	0.67	0 09	0.17	18	19	9	10
Southern Hemisphere	-90	0	-180	180	0.63	0.95	0.46	0.66	0.11	0.17	67	80	38	48
Tropics					0.77	0.97	0.66	0.83	0.10	0.16	48	53	27	35
Tropical continents	-30	30	-180	180	0.69	0.96	0.48	0.66	0.13	0.24	17	22	4	6
Tropical oceans					0.79	0.97	0.68	0.85	0.10	0.15	56	61	57	45
Niño 3	-4	4	-150	-90	0.90	0.98	0.82	0.91	0.26	0.53	97	97	89	91
North Pacific	30	50	150	230	0.81	0.83	0.45	0.56	0.22	0.44	11	4	4	6
North Atlantic	20	50	-60	-20	0.69	0 70	0.30	0.40	0 12	0.36	10	19	2	3
North America	30	70	-125	-75	0.43	0.37	0.16	0.10	0 31	0.89	7	21	3	4
Eurasia	40	70	-10	140	0.39	0.61	0.14	0.19	0.31	0 72	0	11	0	0

Average correlations (1979-1993) are of MSU_{2R} and Atmospheric Model Intercomparison Project observed sea surface temperature (SST) runs. Explained variance is average percentage of variance explained by tropical Pacific SST anomalies. Also given are annual and monthly average rms differences between ECHAM3 and MSU_{2R}.

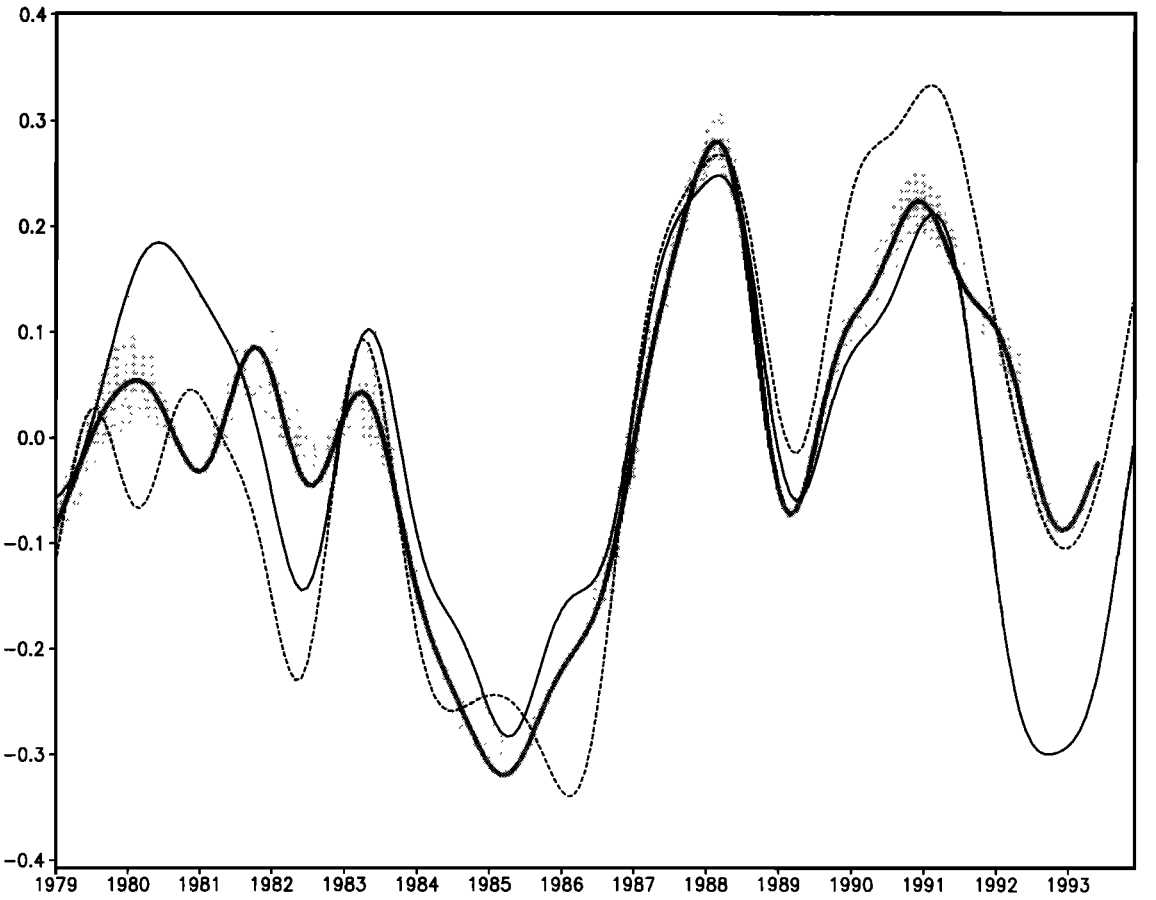

Figure 1. Low-pass-filtered global temperature anomalies of microwave sounding unit (MSU) T_{2R} (solid curve), European Centre for Medium Range Weather Forecasts (ECMWF) reanalyses (stippled wave) and the Hamburg climate model (ECHAM) ensemble simulations. The mean value obtained from the five ECHAM simulations is denoted by the dark gray curve, whereas the shaded area represents this value plus and minus 1 standard deviation of the individual simulations, respectively. Deviations (in Kelvins) are from mean of 1979 - 1992.

peratures are found to remain above the corresponding MSU brightness temperatures for several months after the eruptions of El Chichón and Mount Pinatubo. Since there is no stratospheric aerosol in the model, the question arises as to how these aerosols act on the model troposphere's temperature. This effect will be twofold, indirect and direct. The indirect effect is due to the attenuation of insolation, which will eventually lead to lower SSTs. The strong correlation of SST anomalies and lower tropospheric temperatures will then force a temperature decrease in the model lower troposphere. Besides this indirect (oceanic) effect there is also a direct (atmospheric) effect in response to reduced irradiation. A comparison of model and MSU temperatures is meaningful only in the absence of volcanic aerosol. Therefore the further comparison focuses on the period July 1983 (when the El Chichón aerosol had greatly diminished [see *Christy and McNider*, 1994] to May 1991, which was just before Mount Pinatubo's eruption. This period can be regarded as undisturbed by stratospheric aerosol.

There were no large volcanic events prior to the eruption of El Chichón in April 1982. However, Figure 1 shows less agreement between the anomalies of ECHAM and MSU in 1979 and 1980, the MSU temperatures being systematically higher than those from the model or from surface observations [*Hurrell and Trenberth*, 1996]. In several, but not all regions of the Earth the MSU temperature anomalies are also too warm compared with the ECMWF reanalyses. A closer examination shows that the signal comes mainly from the tropical oceans. It is much weaker in the extratropics and even negative in the North Pacific basin. Possible causes include missing MSU data (such as March 1981) and sampling errors, since NOAA 6 was the only active satellite during most of the time in 1980 and 1981. Furthermore, it was suggested by *Hansen et al.* [1995] that the decrease of stratospheric ozone has greater impact on the troposphere than on the surface. Hence it can be expected that the difference between MSU T_{2R} and surface observations was larger in the early years of the record, when relatively high ozone values were observed. Another cause is the difficulty of creating consistent SST and sea ice data sets, which is discussed in detail, e.g., by *Nomura* [1995]. Grid points with sea ice have to be excluded from the calculation of the anomalies, and temperature differences between the data sets are larger for the earlier years of the period, so that part of the difference between MSU brightness temperatures and model temperatures can be

attributed to uncertainties in the SST fields. Furthermore, 1979 and 1980 had only weak tropical forcing, as indicated by the larger deviations of the individual model runs from the average.

5. Assessment of Regional Predictability

Ensemble integrations allow an estimation of the internal variability of the model and the reproducibility of the results. Predictive skill is limited by the ability of signal reproduction. In this section, different regions of the Earth are investigated by considering the individual experiments.

In Figures 2 and 3, regions of the Earth with high and low predictability, respectively, are presented. Over the tropical land masses (Figure 2), the T_{2R} time series is dominated by large temperature variations connected to ENSO events as well as pronounced temperature drops after the two volcanic eruptions (that both took place in tropical regions). A strong signal is visible during the warm ENSO events, as revealed by the small variations among the five simulations. The reproducibility of the signal is considerably weaker during the cold events, and differences to the ECMWF reanalyses are larger during these periods.

In contrast, Figure 3 shows clearly the different response to boundary forcing in high latitudes compared with the tropics. Whereas the five simulations hardly exhibit any differences in the Niño 3 region (not shown), there are large variations over the extratropical continents, especially over western Europe. While there is a small variation in the average of the five simulations, the variability for each individual member of the ensemble is close to that from the MSU and from the ECMWF reanalysis. There is clearly astounding agreement between the reanalyses and the MSU 2R, though in this region the two data sets are virtually independent.

The North Pacific and the North Atlantic as extratropical regions with high correlations between ECHAM and MSU are of particular interest. There is a distinct cold signal in the Pacific during the ENSO events of 1982 / 1983 and 1987 and probably also 1992 (Figure 4), though the latter temperature curve is influenced by the Mount Pinatubo cooling. A small increase in the MSU temperature record compared with the ECMWF reanalyses can be seen. This trend is absent in the Atlantic, and only a weak, unstable ENSO signal can be identified (not shown).

6. Discussion

Recently, *Christy and McNider* [1994] and *Graham* [1995] stated from observational data that the global average tropospheric temperature is determined by observed ocean surface temperatures, to a large extent, and with an accuracy that is rather close to that achieved by available observing systems like radiosondes. As shown by *Spencer and Christy* [1992a, b, 1993], the correlation of MSU data and conventional observing systems is generally very good. By comparing MSU brightness temperatures with simulated values from the model, one can corroborate and extend these findings which are that in the absence of volcanic aerosol, ECHAM is

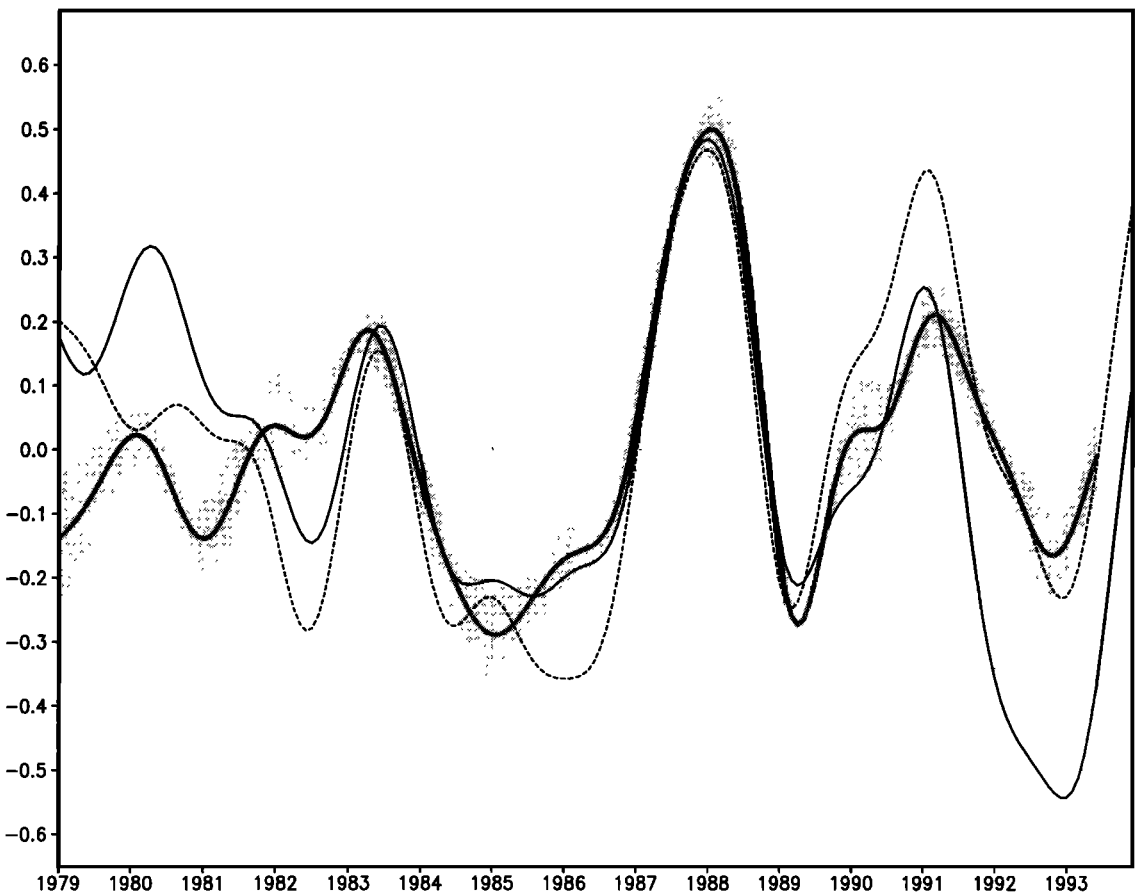

Figure 2. Same as Figure 1, except for tropical land masses (30°S - 30°N).

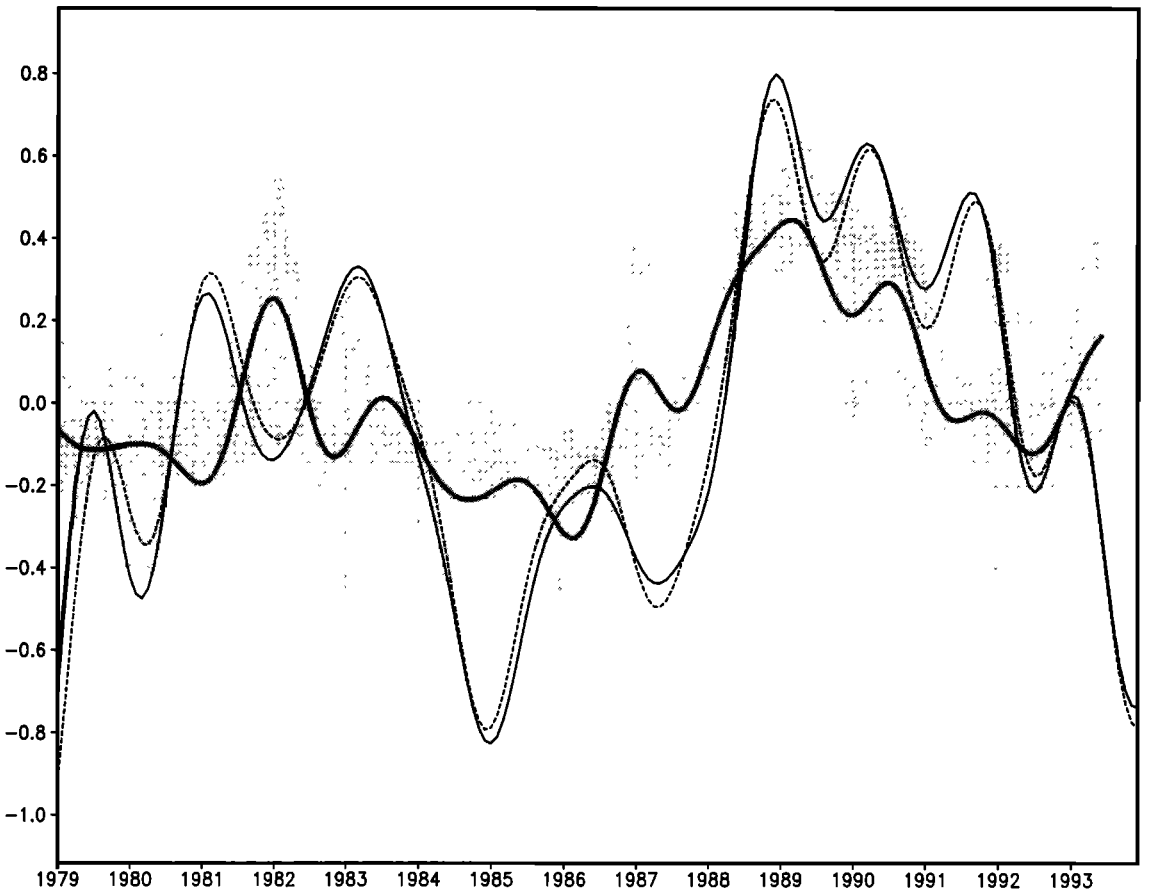

Figure 3. Same as Figure 1, except for Eurasia (40°N - 70°N, 10°W - 140°E).

able to reproduce the atmospheric response to SST anomalies with a high degree of confidence for those regions of the troposphere where the weighting function contributes substantially, i.e., between the surface and ~500 hPa.

Bengtsson et al. [1996] show that ECHAM is able to reproduce the tropical atmospheric response to SST anomalies quite well. The atmospheric circulation in the extratropics is determined, to a great degree, by the large-scale dynamical circulation. Since small differences in the initial state can result in quite different realizations of the atmospheric circulation, the reproducibility of the model integration is expected to be smaller. Nevertheless, there are extratropical regions with a large correlation of T_{2R} and ECHAM3 temperatures, suggesting that SST anomalies play an important role also in parts of the middle and high latitudes and that the model is able to reasonably reproduce large, regional mean tropospheric temperature anomaly patterns forced by these anomalies.

This conclusion gives rise to a number of inferences. The geographical distribution of the correlations suggests that the main SST signal comes from the tropics, as can be seen from the experiment with observed SST forcing only in the tropical Pacific. Only minor differences are found between simulations with observed SST in all tropical oceans (not shown) or just in the Pacific, establishing the well-known finding that it is the tropical Pacific temperatures that determine the global temperature anomalies, to a large extent. Of particular interest is the fact that the correlation over the tropical land masses is of comparable magnitude to that of the oceans, although land surface temperatures are calculated rather than prescribed. It can therefore be expected that a quality improvement of the SST observations in the tropical Pacific (e.g., an increase of the number of observations) will be beneficial for estimating the global atmospheric temperature and quantifying its uncertainties

The high degree of agreement for the recent decade allows, in principle, for an attempt to monitor tropospheric temperatures for periods where observed SSTs (with as much global coverage as possible) are available. Owing to long records of ship observations, this is the case for a period much longer than upper air temperature measurements exist. To assess the effect of different SST data sets, an integration was made using the Meteorological Office Global Sea Ice and Sea Surface Temperature Data Set (GISST) data set of monthly mean observed SST from 1949 on [*Parker et al.*, 1994] with ECHAM3. There is reasonable agreement between the two model simulations with different SSTs from 1982 on (Figure 5). Prior to 1982, larger temperature differences were found. A detailed investigation shows that, to a large extent, these differences are caused by corresponding inconsistencies in the different SST data sets prior to October 1981 (not shown), with differences typically ~0.1 K in the tropical oceans. In limited areas, much larger differences can be found in high latitudes, which are mainly caused by different sea ice cover estimates [see *Nomura*, 1995].

The above considerations allow the possibility of linking physically different quantities, such as surface observations (SST) and satellite soundings (MSU) in relation to each another by means of judging their usefulness as initial conditions for the GCM. Taking into account uncertainties in the historical SST series due to random errors, local sampling errors, and instrumental biases [*Parker et al*, 1994, 1995], it is possible to simulate the vertically inte-

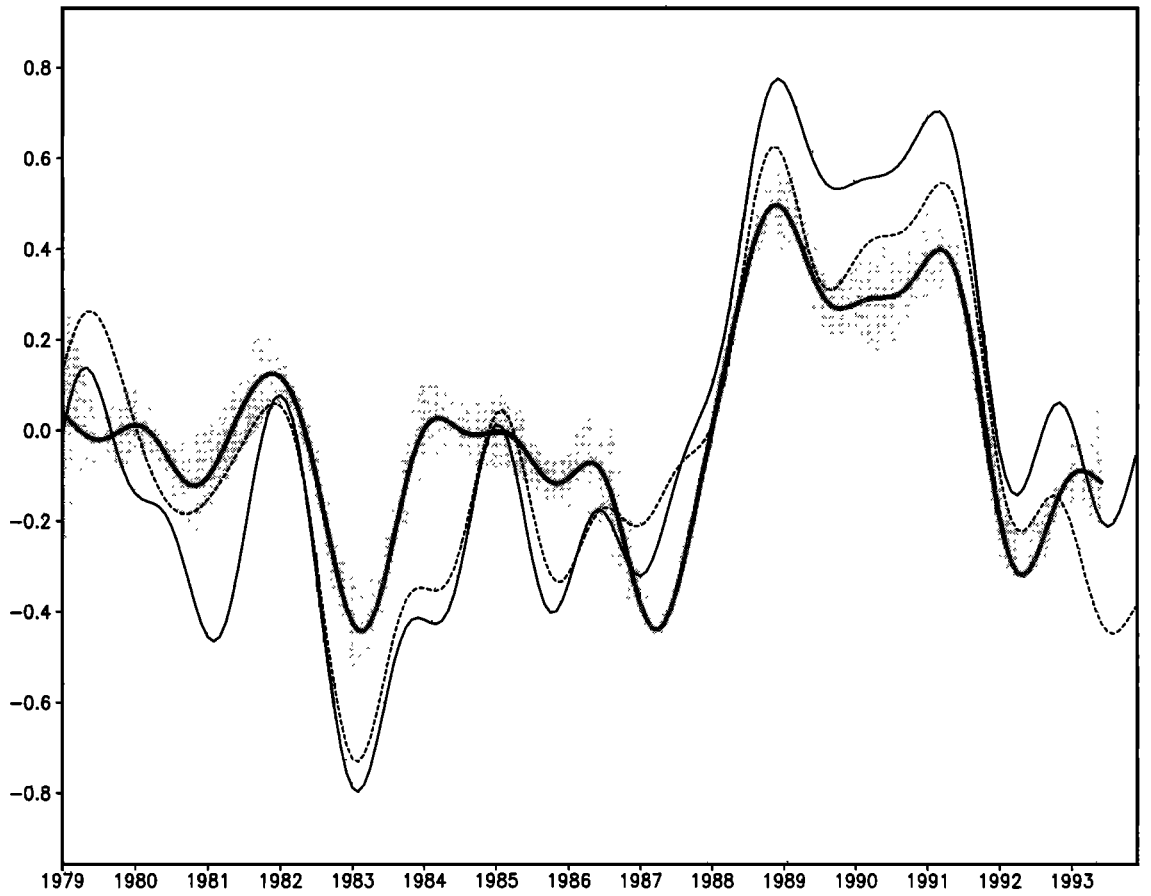

Figure 4. Same as Figure 1, for the North Pacific (30°N - 50°N, 150°E - 130°W).

grated tropospheric temperature with an accuracy of ~0.2 K, as judged from the model response to the different SST series. Going back in time, the SSTs appear to be of only limited use, owing to inadequate data coverage.

Taking GISST as the best given estimate for historic SSTs, the linear least squares global, lower tropospheric temperature trend for the period 1949 to 1993 is +0.08 K/decade. For the tropical belt alone the trend is +0.12 K/decade. There is, however, evidence for an enhanced temperature rise since the mid-1970s (see *Flohn et al.*, 1990).

From Figures 1 and 2 it can be seen that ECHAM and the ECMWF reanalyses are relatively colder compared with the MSU in 1980 and 1981 but warmer after 1990 / 1991. This effect is visible in the tropics, where the agreement of the ECMWF reanalyses with ECHAM and with the MSU record is of comparable magnitude, but not (see Figures 3 and 4) in the extratropics, where there is a close agreement of the MSU and the temperatures from the reanalysis. The causes for this discrepancy are not clear. *Hansen et al.* [1995] and *Hurrell and Trenberth* [1996] discuss possible reasons for the small negative temperature trend in the MSU that is observed, contrary to the surface observations, since 1979. A combination of sampling problems, unresolved sensor drift, and stratospheric ozone decrease effects may be responsible for differences between MSU and ECHAM. However, Figures 3 and 4 show good agreement between the reanalyses and the MSU (although these are not strictly independent, as discussed above). This might point as well toward a possible systematic trend in the SST data set, which would be visible mainly in the tropics.

Answers to this fundamental question may be expected from further investigations, taking carefully into account other sources of global temperature data that could help to minimize uncertainties in the model response. Radiosonde observations are available with reasonable quality for ~30 years; they are highly correlated to MSU temperatures (Table 1). Other sources of interest include the reanalyses from the National Center for Environmental Prediction (NCEP), currently available from 1982 to 1993 but intended to cover the period from the mid-1950s to the present and from NASA's Goddard Space Flight Center, currently available for the period 1985 to 1990. However, preliminary investigations [*Arpe and Stendel*, 1995; *Stendel and Arpe*, 1996] show also discrepancies between the three reanalyses; but, since these only partially cover the same period, this issue must be left to a detailed examination.

The information in Figures 3 and 4 points to another possibility for the discrepancy between reanalysis and MSU data. As mentioned earlier, the MSU 2R data are carefully intercalibrated from one spacecraft to the next so that a homogeneous time series is generated. No outside data (i.e., radiosondes) are used in the construction of the MSU products. However, the operational satellite data, utilized in reanalysis primarily over oceanic regions, have not been subjected to these precise intercalibrations. Therefore it is possible that biases between satellite instrumentation remain in the operational products because they are small, of the order of only a few tenths of a degree. However, for global mean quantities and decadal trends these small biases are actually larger than the variations being sought. Therefore, for large-scale mean quantities

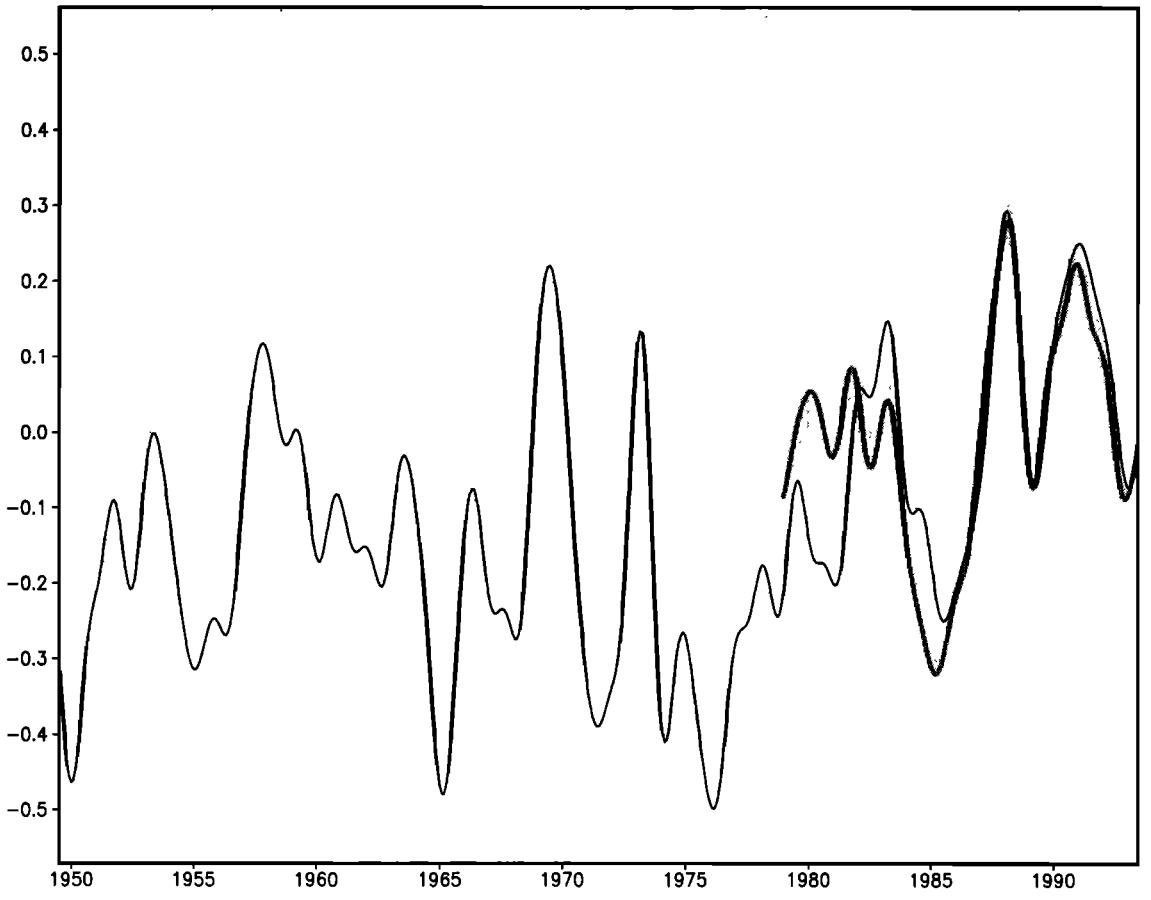

Figure 5. Low-pass-filtered global temperature anomalies of ECHAM ensemble simulations with Meteorological Office Global Sea Ice and Sea Surface Temperature Data Set (GISST) sea surface temperature (SST) for 1949 - 1993 (solid curve) and Atmospheric Model Intercomparison Project (AMIP) SST for 1979 - 1993. The mean value obtained from the five AMIP simulations is denoted by the gray curve, whereas the shaded area represents this value plus and minus 1 standard deviation of the individual simulations, respectively. Deviations (in Kelvins) are from mean of 1979 - 1992.

and trends, the reanalyses may still contain small but important errors over regions that rely primarily on operational satellite soundings. Evidence for such a finding is shown in the relatively large differences between reanalysis and MSU in Figure 2, an oceanic region, and the very small differences in Figure 3, which is a region of dense radiosonde coverage.

7. Conclusions

Interannual tropospheric temperature variations are determined, to a large extent, by the SST distribution. The ECHAM model is able to reproduce the globally averaged temperatures of the troposphere with a high degree of accuracy. Largest agreement with MSU brightness temperatures is found in the tropics and generally in areas where the temperature variance is small, i.e., over a large part of the world ocean. In general, these are regions that lack traditional observing systems such as radiosondes. Therefore GCMs like ECHAM can be valuable for monitoring the temperature of the lower troposphere with an accuracy comparable to that of available observation systems for basin-averaged quantities. This provides the ability to discern anthropogenic climate modification with a greater degree of confidence, since there is evidence that climatic response to greenhouse gas increases will be largest in the tropics and in the upper troposphere, where only a limited number of traditional observations is available [*Flohn et al.*, 1990]. With the discussed restrictions concerning the quality of SST records, the model can be used to gain information about the temperature trends in greenhouse-gas-relevant levels.

Moreover, the method described in this paper allows one to judge the quality of physically different variables in relation to each another by considering them as initial conditions for the GCM. This allows statements, e.g., about the quality of SST and sea ice estimations. We have shown that there is an inconsistency between the SST and MSU temperatures. Taking into account additional data sets, like radiosonde observations or reanalyses, in the described way would enable us to obtain a more comprehensive and consistent view of tropospheric temperature trends.

Large regional differences are visible, indicating that temperature variability is due to different reasons. In the tropics, coupling between different scales is essentially linear and strongly driven by the release of latent heat. The ECHAM model is able to represent this kind of temperature variation with a great degree of accuracy. In contrast, dynamical instability is common to the extratropical circulation, so that the effect of SST on tropospheric temperatures is essentially nonlinear [*Bengtsson et al.*, 1996]. The incorporation of an ensemble of climate simulations, using slightly different initial states, will add a measure of confidence also in the monitoring of extratropical temperatures, although an ensemble of more than five experiments may have to be chosen.

Acknowledgments. The MSU data used in this study were provided by John Christy and Roy Spencer. We thank David Parker from UKMO for providing us with the GISST data set. We are indebted to Rex Gibson, Per Kållberg, Sakari Uppala, and Atsushi Nomura from ECMWF for making available the reanalysis data and for discussions on possible causes for differences between the analyses. Thanks are extended to the anonymous reviewers of this manuscript, whose comments helped to clarify and improve the text. We are also grateful to our colleagues at the Max-Planck-Institut für Meteorologie in Hamburg and at the German Climate Computing Centre for technical support and discussions. This study has been supported by the EC under contract EV5V-CT93-0286 and by the BMBF project 07 VKV01 1/1.

References

Angell, J K., Variations and trends in tropospheric and stratospheric global temperatures, 1958-87, *J. Clim.*, *1*, 1296-1313, 1988.

Angell, J.K., Variations in global tropospheric temperature after adjustment for the El Niño influence, 1958-1989, *Geophys. Res. Lett.*, *17*, 1093-1096, 1990.

Arpe, K., and M. Stendel, Evaluation of the ECMWF re-analysis with emphasis on the precipitation, paper presented at 20th Climate Diagnostic Workshop, Seattle, Wash., Oct. 23-27, 1995.

Bengtsson, L , and J. Shukla, Integration of space and in situ observations to study global climate change, *Bull. Am. Meteorol. Soc.*, *69*, 1130-1143, 1988.

Bengtsson, L., K. Arpe, E. Roeckner, and U. Schulzweida, Climate predictability experiments with a general circulation model, *Clim. Dyn.*, *12*, 261-278, 1996.

Bjerknes, J., Atlantic air-sea interaction, in *Advances in Geophysics*, pp. 1-82, Academic, San Diego, Calif., 1964.

Boer, G.J., N A. McFarlane, and M. Lazare, Greenhouse-gas induced climate change simulated with the CCC second-generation general circulation model, *J. Clim.*, *5*, 1045-1077, 1992.

Cayan, D.R., Latent and sensible heat flux anomalies over the northern oceans: The connection to monthly atmospheric circulation, *J. Clim.*, *5*, 354-369, 1992a.

Cayan, D.R., Latent and sensible heat flux anomalies over the northern oceans: Driving the sea surface temperature, *J. Phys. Oceanogr.*, *22*, 859-881, 1992b.

Christy, J.R., Temperature above the surface layer, *Clim. Change*, *31*, 455-474, 1995.

Christy, J.R., and S.J. Drouilhet, Variability in daily, zonal mean lower stratospheric temperatures, *J. Clim.*, *7*, 106-120, 1994.

Christy, J.R., and R.T. McNider, Satellite greenhouse signal, *Nature*, *367*, 325, 1994

Christy, J.R., R.W. Spencer, and R.T. McNider, Reducing noise in the daily MSU lower tropospheric temperature data set, *J. Clim.*, *8*, 888-896, 1995.

Flohn, H., A. Kapala, H.R. Knoche, and H. Mächel, Recent changes of the tropical water and energy budget and of midlatitude circulations, *Clim. Dyn.*, *4*, 237-252, 1990.

Franklin, B., Meteorological imaginations and conjectures, *Manchester Liter and Philos. Soc. Mem. and Proc.*, *2*, 122, 1784.

Gates, W.L., AMIP: The atmospheric model intercomparison project, *Bull. Am Meteorol Soc.*, *73*, 1962-1970, 1992.

Graham, N.E., Simulation of recent global temperature trends, *Science*, *267*, 666-671, 1995.

Hansen, J., H. Wilson, M. Sato, R. Ruedy. K. Shah, and E. Hansen, Satellite and surface temperature data at odds?, *Clim. Change*, *30*, 103-117, 1995

Hoerling, M.P., M.L. Blackmon, and M.-F. Ting, Simulating the atmospheric response in the 1985-87 El Niño cycle, *J. Clim.*, **5**, 669-682, 1992

Hurrell, J.W., and K.E. Trenberth, An evaluation of monthly mean MSU and ECMWF global atmospheric temperatures for monitoring climate, *J Clim.*, *5*, 1424-1440, 1992

Hurrell, J.W. and K.E. Trenberth, Satellite versus surface estimates of air temperature since 1979, *J. Clim.*, *9*, 2222-2232, 1996.

Intergovernmental Panel on Climate Change (IPCC), *Climate Change 1992: The Supplementary Report to the IPCC Scientific Assessment*, edited by J.T. Houghton, B.A. Callander and S.K. Varney, 200 pp., Cambridge Univ. Press, New York, 1992.

IPCC, *Climate Change 1995: The Science of Climate Change*, edited by J.T. Houghton, L.G. Meira Filho, B.A. Callander, N. Harris, A. Kattenberg and K. Maskell, 572 pp., Cambridge Univ. Press, New York, 1996.

Kushnir, Y., Interdecadal variations in North Atlantic sea surface temperature and associated atmospheric conditions, *J. Clim.*, *7*, 141-157, 1994.

Labitzke, K., and M.C. McCormick, Stratospheric temperature increase due to Pinatubo aerosols, *Geophys. Res. Lett.*, *19*, 207-210, 1992

Lau, N.-C., Modeling the seasonal dependence of the atmospheric response to observed El Niños in 1962-76, *Mon. Weather Rev.*, *113*, 1970-1996, 1985.

Manabe, S., R.J. Stouffer, M.J. Spelman, and K. Bryan, Transient responses of a coupled ocean-atmosphere model to gradual changes of atmospheric CO_2, I; Annual mean response, *J. Clim.*, *4*, 785-818, 1991.

Newell, R.E., and B.C. Weare, Ocean temperatures and large scale atmospheric variations, *Nature*, *262*, 40-41, 1976a.

Newell, R.E., and B.C. Weare, Factors governing tropospheric mean temperature, *Science*, *194*, 1413-1414, 1976b.

Nomura, A., Global sea ice concentration data set for use with the ECMWF re-analysis system, Tech. Report *47*, 25 pp., Eur. Cent. for Medium-Range Weather Forecasts, Reading, England, 1995.

Oort, A.H., and H. Liu, Upper-air temperature trends over the globe, 1958-1989, *J. Clim* , *6*, 292-307, 1993.

Pan, Y.H., and A.H. Oort, Global climate variations connected with sea surface temperature anomalies in the eastern equatorial Pacific Ocean for the 1958-1973 period, *Mon. Weather Rev.*, *111*, 1244-1258, 1983.

Parker, D.E., P.D. Jones, C.K. Folland, and A.Bevan, Interdecadal changes of surface temperature since the late nineteenth century, *J. Geophys. Res.*, *99*, 14,373-14,399, 1994

Parker, D.E., C.K. Folland, and M. Jackson, Marine surface temperature: Observed variations and data requirements, *Clim. Change*, *31*, 559-600, 1995

Pedersen, K., T. Ese, and I. Kaneström, Persistent anomalies of sea-surface temperature in the North Atlantic, *Z. Meteorol.*, *40*, 229-234, 1990.

Prabhakara, C., J.J. Nucciarone, and J.-M. Yoo, Examination of global atmospheric temperature monitoring with satellite microwave measurements, 1, Theoretical considerations, *Clim. Change*, *30*, 349-366, 1995.

Prabhakara, C., J.-M. Yoo, S.P. Maloney, J.J. Nucciarone, A. Arking, M. Cadeddu, and G. Dalu, Examination of global atmospheric temperature monitoring with satellite microwave measurements, 2, Analysis of satellite data, *Clim. Change*, *33*, 459-476, 1996a.

Prabhakara, C., M. Cadeddu, J.-M. Yoo, A. Arking, and G. Dalu, Examination of global atmospheric temperature monitoring with satellite microwave measurements, 3, Cloud and rain contamination, *Clim. Change*, *33*, 491-496, 1996b.

Reynolds, R.W., A real-time global sea surface temperature analysis, *J. Clim.*, *1*, 75-86, 1988.

Roeckner, E., et al., Simulation of the present-day climate with the ECHAM model: Impact of model physics and resolution, *Rep. 93*, 172 pp. Max-Planck-Inst. for Meteorol., Hamburg, Germany, 1992.

Shah, K P., and D. Rind, Use of microwave brightness temperatures with a general circulation model, *J. Geophys. Res.*, *100*, 13,841-13,874, 1995.

Spencer, R.W., and J.R. Christy, Precision and radiosonde validation of satellite gridpoint temperature anomalies, I, MSU channel 2, *J. Clim.*, *5*, 847-857, 1992a

Spencer, R.W., and J.R. Christy, Precision and radiosonde validation of satellite gridpoint temperature anomalies, II, A tropospheric retrieval and trends during 1979-90, *J. Clim.*, *5*, 858-866, 1992b.

Spencer, R.W., and J.R. Christy, Precision lower stratospheric temperature monitoring with the MSU: Validation and results 1979-91, *J. Clim.*, *6*, 1194-1204, 1993.

Spencer, R.W., J.R. Christy, and N.C. Grody, Global atmospheric temperature monitoring with satellite microwave measurements: Method and results 1979-84, *J. Clim.*, *3*, 1111-1128, 1990.

Spencer, R.W., J.R. Christy and N.C. Grody, Analysis of 'Examination of global atmospheric temperature monitoring with satellite microwave measurements', *Clim. Change*, *33*, 477-489, 1996.

Stendel, M., and K. Arpe, Evaluation of the hydrological cycle in reanalyses and observations, paper presented at the Second International Scientific Conference on the Global Energy and Water Cycle, Washington, D.C , June 17-21, 1996.

Trenberth, K.E., J.R. Christy, and J.W. Hurrell, Monitoring global monthly mean surface temperatures, *J. Clim.*, *5*, 1405-1423, 1992.

Wallace, J.M., C. Smith, and Q.-R. Jiang, Spatial patterns of atmosphere/ocean interaction in the northern winter, *J. Clim.*, *3*, 990-998, 1990.

L. Bengtsson and M. Stendel, Max-Planck-Institut für Meteorologie, Bundesstr. 55, D-20146 Hamburg, Germany. (e-mail: bengtsson@dkrz.de; stendel@dkrz.de)

(Received April 22, 1996; revised June 2, 1997;
accepted June 4, 1997.)